WIRE DRAWING IN DIE-LESS CONICAL PRESSURE UNIT

Dr. Yassr Y. Kahtan, Asst. Prof. Talal Y. M. Al-Naib

Abstract— A theoretical study of the die-less wire drawing was carried out in which the conventional die is replaced by a die-less conical orifice reduction unit. The process involves pulling the wire through the conical die-less unit which is filled with a polymer melt, the pulling action causes yielding of the continuum and a reduction in area is then obtained. A Newtonian behavior of the polymer melt and a rigid non-linear strain-hardening continuum were considered in which non-linear equations are formulated for the pressure and the stress increment in the die unit. A finite difference numerical technique was applied to solve these equations for the plasto-hydrodynamic pressure and the stress, which enabled prediction of the non-linear deformation profile of the continuum, the pressure distribution, and the percentage reduction in area for various drawing speeds. The maximum reduction in area for wire drawing is (5.5%). The maximum pressure lies in the rear half of the die unit for various drawing speeds and it was found to be larger than that obtained by previous experimental work, however the drawing stress attained in this technique was less than that obtained using conventional dies.

Index Terms— Wire Drawing, Die-less, Hydrodynamic Pressure.

1 INTRODUCTION

Wire drawing operation involves pulling metal through a die by means of a tensile force applied to the exit side of the die. The material within the die is rendered plastic by the combined action of the applied longitudinal pull and the pressure developed between the wire and the die [1].

The reduction in diameter of a solid bar or rod by successive drawing is known as bar, rod, or wire drawing, depending on the diameter of the final product. In addition to direct application such as electrical wiring, wire is the starting material for many products including wire frame structures (ranging from coat hangers to shopping carts), nails, screws, bolts, rivets, wire fencing, etc.

In this technique, the wire is pulled through a tubular orifice of conical or stepped bore shape, which is filled with viscous fluid as shown in figure (1). Experiments [2] have shown that products having comparable dimensional and surface qualities can be achieved using this method. The only limitation observed during this process was the decrease in the reduction of the wire diameter at higher drawing speeds [3].

2 THEORETICAL ANALYSIS

This study is focused on die-less wire drawing, the pressure medium is considered Newtonian. Non-linear equations are formulated for the pressure and axial stress increment in a conical tubular orifice with viscous fluid through which a circular cross-section continuum is being pulled. A finite difference numerical technique was applied to solve these equations for the plasto-hydrodynamic pressure and the resulting axial stress, which in turn enabled prediction of the non-linear deformation profile of the continuum, the pressure distribution and the percentage reduction in area for various drawing speeds. mechanism that can perform planar biaxial loading, the composite materials laminates, preparation of the required specimens, investigation of their mechanical properties, fatigue behavior under uniaxial and plane biaxial loading.

There is no standard shape or design for the biaxial specimens until now [4], so the specimen design was based on the generic form shown in fig (1), with specimen arms all of the same length and a circular central gauge section.

2.1 ANALYSIS PRIOR TO THE DEFORMATION OF DIE-LESS WIRE DRAWING PROCESS

Figure (2) shows the geometrical configuration of the orifice and the continuum, the gap at any point is given by:

$$h = h_1 - kx \qquad (1)$$

Where,

$$k = (h_1 - h_2)/B$$

k = is the slope of the die.

B = is the length of the die unit.

h_1 = is the radial gap at the die entry.

h_2 = is the radial gap at the die exit.

h = is the radial gap at any point in the die.

x = is any distance (point) in the die.

The pressure gradient within the gap for a Newtonian fluid medium may be proven and expressed as:

$$\frac{\partial P}{\partial x} = \frac{\partial \tau}{\partial y} \qquad (2)$$

And the shear stress as:

$$\tau = \mu \frac{\partial u}{\partial y} \qquad (3)$$

The pressure at any point (x) within the orifice may be expressed by:

$$P = \frac{6\mu v}{k}[\{\frac{1}{(h_1 - kx)} - \frac{h_0}{2(h_1 - kx)^2}\} - \{\frac{1}{h_1} - \frac{h_0}{2h_1^2}\}] \qquad (4)$$

Where, (P) is the hydrodynamic pressure exerted on the continuum. However (h_0) is still not determined. Using the boundary condition that P = 0 at x = B where (h_1-kx) = h_2 in equation (4) and rearranging:

$$h_0 = \frac{2h_1 h_2}{(h_1 + h_2)} \qquad (5)$$

The expression for the shear stress at any depth in the fluid may be obtained as:

$$\tau = \frac{1}{2}(\frac{\partial P}{\partial x})(2y - h) - \mu \frac{v}{h} \qquad (6)$$

At the surface of the continuum the shear stress (τ_x) is obtained by putting y = 0 in equation (6), thus:

$$\tau_x = -\frac{h}{2}(\frac{\partial P}{\partial x}) - \mu \frac{v}{h} \qquad (7)$$

After substituting for ($\partial P / \partial x$), (h) from equation (1), and rearranging terms thus becomes:

$$\tau_x = \mu v[\frac{3h_0}{(h_1 - kx)^2} - \frac{4}{(h_1 - kx)}] \qquad (8)$$

This shear stress gives rise to drag force on the continuum and at a point (x) within the orifice this may be expressed as:

$$F_d = \int \pi D_1 \tau_x dx = \pi D_1 \mu v \int [\frac{3h_0}{(h_1 - kx)^2} - \frac{4}{(h_1 - kx)}]dx$$

where, (F_d) is the drag force, (D_1) is the wire diameter before deformation. After integrating and noting that at x = 0, F_d = 0, yields:

$$F_d = \pi D_1 \frac{\mu v}{k}[\frac{3h_0}{(h_1 - kx)} - \frac{3h_0}{h_1} + 4\ln\{\frac{(h_1 - kx)}{h_1}\}] \qquad (9)$$

The axial stress developed in the continuum is thus:

$$\sigma_x = \frac{4F_d}{\pi D_1^2} = \frac{4\mu v}{D_1 k}[3h_0\{\frac{1}{(h_1 - kx)} - \frac{1}{h_1}\} + 4\ln\{\frac{(h_1 - kx)}{h_1}\}] \qquad (10)$$

Where, (σ_x) is the axial pulling stress in the wire.

ISSN 2229-5518

2.2 Analysis of Deformation Zone of Die-Less Wire Drawing Process

2.2.1 Plastic Deformation

The combined effects of the axial stress and the hydrodynamic pressure will cause plastic yielding of the continuum at any point (x), within the orifice as soon as the plastic yield criterion becomes satisfied. If the material of the continuum is assumed to be rigid non-linearly strain hardening such that the flow stress could be expressed as:

$$Y = Y_e + A\varepsilon^n \qquad (11)$$

Where, (Y) is the yield stress, (Y_e) is the initial yield stress, (A) is the material constant, (ε) is the strain, (n) is the strain hardening index.

Then according to the Tresca yield criterion, plastic yielding will commence at a point (x_p), provided that:

$$P + \sigma_x = Y_e \qquad (12)$$

Once plastic yielding is predicted to commence for given values of (μ), (v) and the geometrical parameters of the orifice, further permanent deformation of the continuum should continue to take place as long as:

$$P + \sigma_x \geq Y = Y_e + A\varepsilon^n \qquad (13)$$

is satisfied at any distance from (x_p).

2.2.2 Pressure in the Deformation Zone

In the deformation zone the pressure gradient is slightly different, and can be expressed as:

$$\frac{\partial P}{\partial x} = 6\mu\left(\frac{v}{h^2} - \frac{v_0 h_0}{h^3}\right) \qquad (14)$$

Where (v_0) is the speed of the continuum at the position of maximum pressure ($c = -v_0h_0$). Equation (14), when expressed in finite difference form, gives pressure values at different points at a distance (Δx) apart. It may be reasonable to assume that the plastic deformation takes place in a straight-line profile over small length (Δx). Thus:

$$P_i = P_{i-1} + 6\mu\Delta x\left(\frac{v_i}{h_i^2} - \frac{v_0 h_0}{h_i^3}\right) \qquad (15)$$

Where,

$$h_i = h_{i-1} - (k - b_i)\Delta x \qquad (16)$$

$$v_i = v_{i-1}(D_{i-1} / D_i)^2 \qquad (17)$$

$$D_i = D_{i-1} - 2b_i\Delta x \qquad (18)$$

Where, (b_i) is the non-linear deformation profile slope of the continuum.

2.2.3 Axial Stress in the Deformation Zone

Referring to figure (3) which show an element of the continuum within a straight conical profile, the increment in axial stress may be expressed as:

$$d\sigma_x = -2\frac{dD}{D}(Y + \tau_x \cot\alpha) \qquad (19)$$

Where (α) is the semi-angle of the conical deformation profile. But the diameter ($D = D_1 - 2bx$) is such that ($dD = -2bdx$) and ($\cot\alpha = -1/b$).

Now from equation (7), the shear stress (τ_x) is given by:

$$\tau_x = -\frac{h}{2}\left(\frac{\partial P}{\partial x}\right) - \mu\frac{v}{h}$$

Substituting for ($\partial P/\partial x$) from equation (14) and rearranging:

$$\tau_x = -\frac{\mu}{h}\left(4v - \frac{3v_0 h_0}{h}\right)$$

2.2.4 Analysis after the Deformation Has Ceased

The deformation of the wire ceases completely at some distance before the exit of the die-less reduction unit, taking a final shape (diameter) to the wire. In order to determine the pressure in this region, the analysis of this region is similar to that before the deformation begins, thus:

$$P = \frac{6\mu v}{k}\left[\left\{\frac{1}{(h_1 - kx)} - \frac{h_0}{2(h_1 - kx)^2}\right\} - \left\{\frac{1}{h_1} - \frac{h_0}{2h_1^2}\right\}\right] \quad (21)$$

The final value for (v) is used in equation (21) and (x) is any distance after the deformation has ceased.

In summary, the procedure for predicting the theoretical results, involves the determination of (x_p), the distance from the die entry of the reduction unit to where plastic deformation commences, by iterative computation of equation (12) in conjunction with equations (4), (5), and (10).

Substituting for (τ_x), ($\cot\alpha$), and (dD) in equation (19), it becomes:

$$d\sigma_x = \frac{4bdx}{D}\left\{Y + \frac{\mu}{bh}\left(4v - \frac{3v_0 h_0}{h}\right)\right\}$$

This is written in finite difference form as:

$$\sigma_{xi} = \sigma_{xi-1} + \frac{4b_i}{D_i}\Delta x\left\{Y_i + \frac{\mu}{b_i h_i}\left(4v_i - \frac{3v_0 h_o}{h_i}\right)\right\} \quad (20)$$

Where,

$$Y_i = Y_e + A\left\{\ln\left(\frac{D_1}{D_i}\right)^2\right\}^n$$

From this point until the deformation is stopped, the extent of plastic deformation is calculated on the basis of equation (13) when combined with equations (15), and (20) for small increment (Δx) from (x_p). The current slope of the deformation profile (b_i) is determined by iterative computation of equation (13), the current diameter being then given by equation (18).

After the deformation has ceased the pressure can be determined from equation (21).

3 Discussions of Results

A rigid non-linear strain hardening continuum and a Newtonian plasto-hydrodynamic analysis of the die-less unit is carried out.

A finite difference numerical technique is used to determine the pressure distribution, the coat thickness, and the resulting non-linear deformation profile of the drawn continuum.

3.1 Pressure Distribution

The pressure is a very important parameter in the process of die-less wire drawing, because the pulling action of the wire through the viscous fluid generates hydrodynamic pressure and gives rise to drag force. Depending on the type of the fluid and the unit, the combined effect of the pressure and the drag force can be sufficient to cause plastic yielding and subsequently to deform the wire permanently [4]. The pressure verses location through the die at drawing speeds of (0.5-4 m/s) is shown in figure (4). From the figure, it can be seen that as the drawing speed increases the maximum pressure also increases. For all speeds the pressure starts and ends at zero value (atmospheric pressure), and at the same location. The pressure distribution obtained by Hashmi [3] similar conditions had the same trend. However the maximum pressure obtained by Hashmi [3] was lower than that in figure (4). The maximum pressure was found to be (83.26 MPa) at a drawing speed of (0.5 m/s) and (119.68 MPa) at a drawing speed of (1 m/s), whereas Hashmi [3] found that the maximum pressure was (82 MPa) at a drawing speed of (0.5 m/s) and (106 MPa) at a drawing speed of (1 m/s). It can be seen from figure (4) and figure (5), that the plastic deformation starts and ends in the wire before the pressure reached its maximum value for various drawing speeds. This can be justified by knowing that as the wire is deformed a larger gap is then induced in the die unit. The newly added space in the die will be filled with the viscous fluid that needs a greater pressure to continue the polymer melt flow through the die.

3.2 Deformation Profile

The non-linear deformation profile of the wire is shown in figure (5) for various drawing speed (0.5-4 m/s). From the figure it can be seen that as the drawing speed increases the deformation in the wire increases. Figure (5) shows the commencement of yield in the wire which is identical to that obtained by Hashmi [3]. Referring to the figure, the yield starts at a distance of (31.825 mm) from the entry at a drawing speed of (0.5 m/s) and at a distance of (12.317 mm) from the entry at a drawing speed of (2 m/s), while Hashmi [3] located the start of yield at a distance of (31.5 mm) from the entry at a drawing speed of (0.5 m/s) and at a distance of (12.1 mm) from the entry at a drawing speed of (2 m/s). The non-linear deformation profile of the wire obtained is identical to that obtained by Hashmi [3]. Hashmi however obtained a greater reduction in area than that obtained from figure (5). Hashmi found that about (24) percent reduction in area was produced at a drawing speed of (1 m/s) and which increased to about (36) percent reduction in area at a drawing speed of (4 m/s), while from figure (5) about (0.86) percentage reduction in area is obtained at a drawing speed of (1 m/s) and which increases to about (5.5) percent reduction in area at a drawing speed of (4m/s). Experimental results [2] show that about (23) percentage reduction in area was obtained at a drawing speed of about (0.21 m/s) and thereafter rapidly decreases down to about (6) percent reduction in area and remains unchanged for drawing speeds in excess of (2 m/s). This discrepancy can be attributed mainly to the fact that some constants in the deformation zone and the exact position of maximum pressure at various drawing speeds were not clearly given.

3.3 Influence of the Drawing Speed

The drawing speed of the wire material has a great effect on all of the parameters, and it may be considered the most important parameter in the die-less wire drawing process. It can be seen from figure (5), that as the drawing speed is increased the reduction ratio and the coat thickness of the polymer melt on the wire also increase. It was found [3] that further reduction in area would not occur in the wire when the drawing speed was in excess of (2 m/s). A certain range of the drawing speed could be used in order to assure the optimum performance of the die-less drawing process.

4 Conclusions

A theoretical analysis for drawing wire and tube using a novel technique in which a die-less reduction unit in conjunction with a polymer melt is presented.

The main conclusions can be summarized as follows:

1. The plastic deformation starts and ends in the wire and tube before the pressure reaches its maximum value.

2. The deformation profile of the wire (or tube) inside the die-less reduction unit is non-linear and the

ISSN 2229-5518

deformation starts at a distance from the die entry and ends at a distance before the die exit. As the drawing speed increases the deformation range decreases.

3. The drawing stress attained in this technique is less than that obtained using conventional dies. A drawing stress of about (48 MPa) at a drawing speed of (0.5 m/s) for wire is needed by the die-less reduction technique, while a drawing stress [5] of about (190 MPa) is needed for the same conditions in a conventional reduction unit.

5 References

[1] J. Chakrabarty, "Applied Plasticity", Springer. Verlag Inc. New York, 2000.

[2] M.S.J. Hashmi, G.R. Symmons, and H. Parvinmehr, "A Novel Technique for Wire Drawing", J. of Mech. Eng. Sci.Vol. 24,PP.1-4, 1982.

[3] M.S.J. Hashmi, and G.R. Symmons,"A Numerical Solution for the Plasto-Hydrodynamic Drawing of Rigid Non-Linearly Strain Hardening Continuum through a Conical Orifice", Proc. 2nd. Int. Conf. On Numerical Methods for Non-Linearly Problems, Spain,PP.1048-1059, 1984.

[4] M.S.J. Hashmi, "A Note on the Prospects of Plasto-Hydrodynamic Die-Less Tube Sinking", J. of Mech. Working Tech. Vol. 11,PP.237-242 1985.

[5] M.S.J. Hashmi, R. Carmpton, and G.R. Symmons," Effects of Strain Hardening and Strain Rate Sensitivity of the Wire Material during Drawing under Non-Newtonian Plasto-Hydrodynamic Lubrication Conditions", Int. J. Mech. Tool. Des. Vol. 21,PP.71-86, 1981.

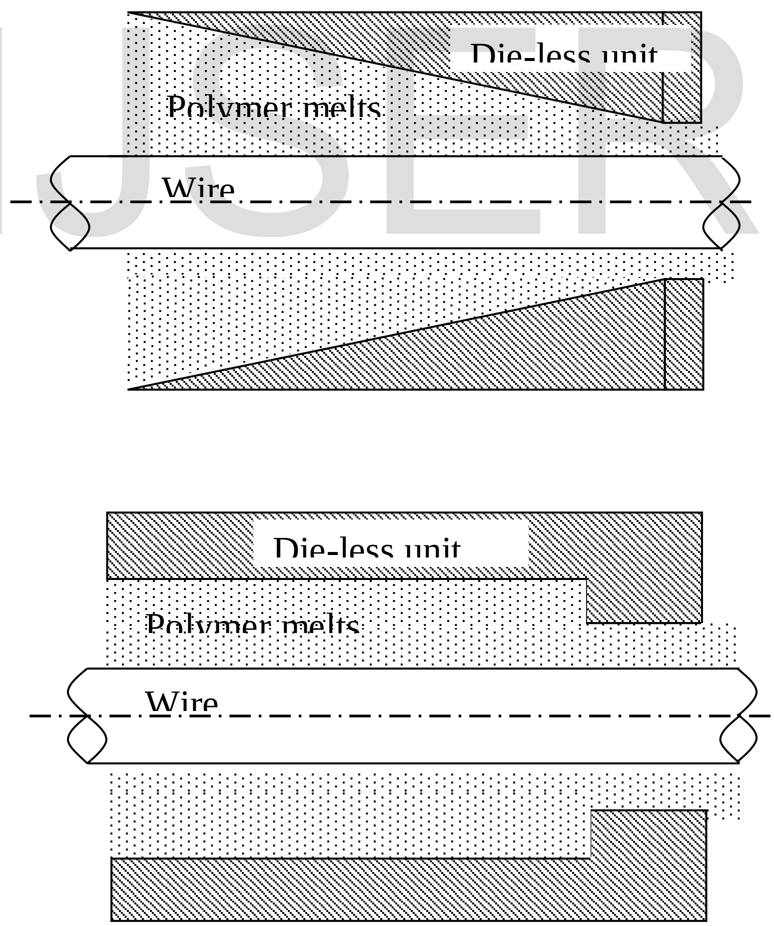

FIGURE (1) SCHEMATIC DIAGRAM SHOWING (A) THE TAPERED BORE

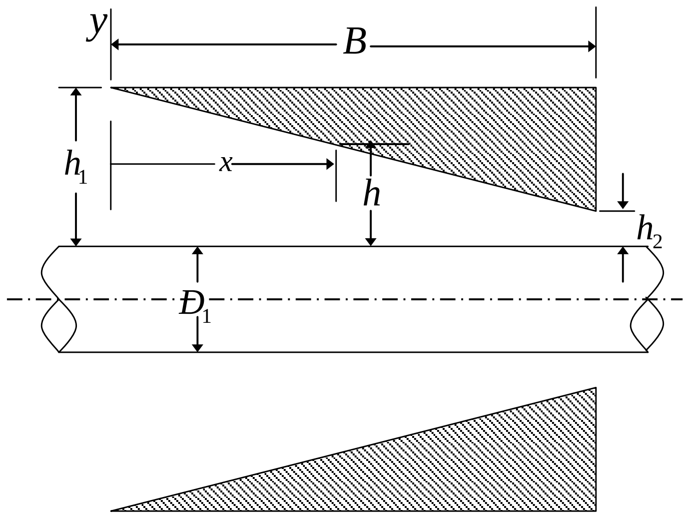

Figure (2) Schematic diagram showing the die-less reduction unit used in the analysis.

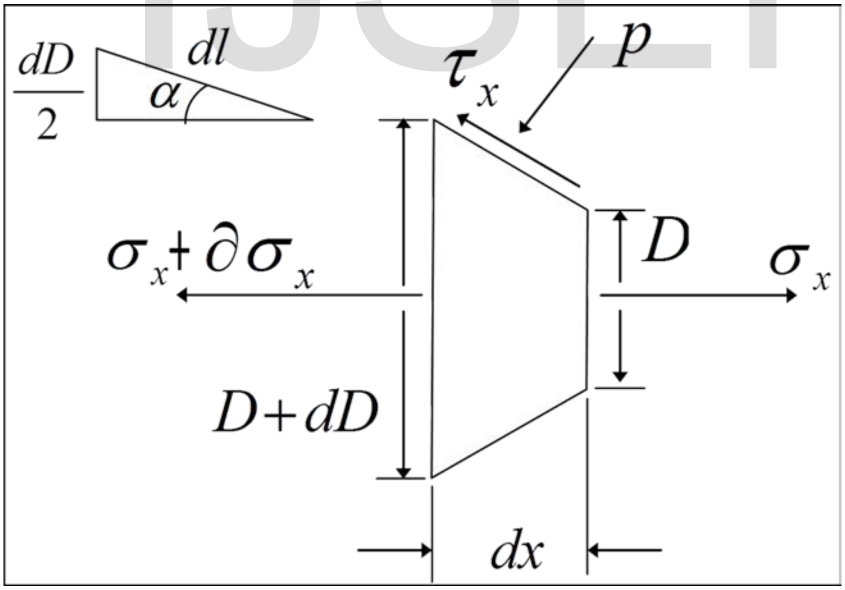

Figure (3) An element in the deformation zone of the wire showing the stresses acting on it.

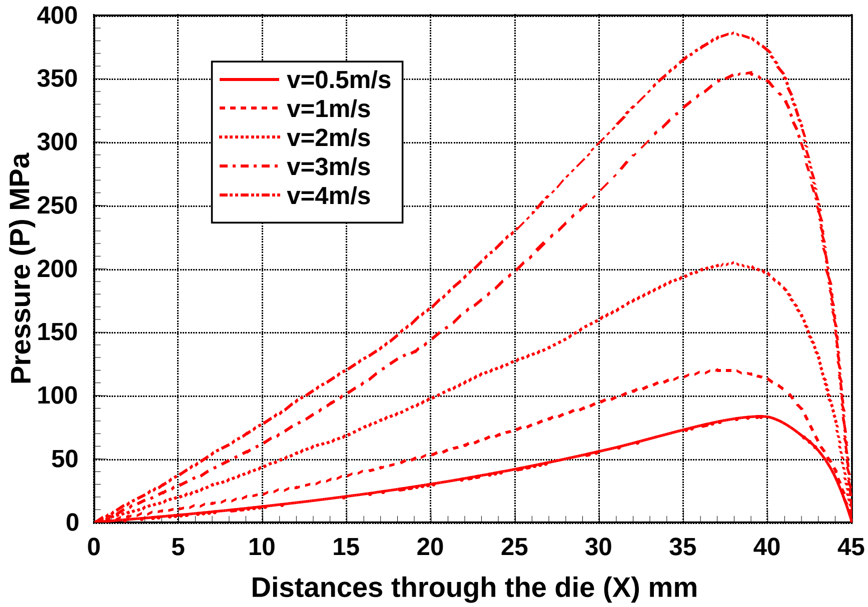

Figure (4) Pressure distribution for wire drawing through a conical die with polymer melt ($\mu = 120$ N.s/m^2) at different drawing speeds.

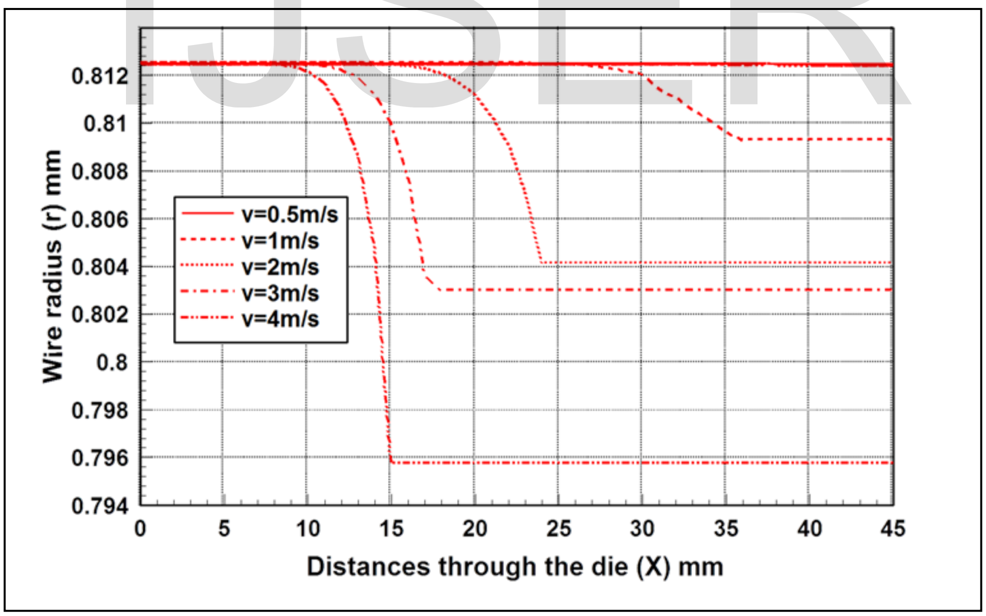

Figure (5) Non-linear deformation profile for wire drawing through a conical die with polymer melt ($\mu = 120$ N.s/m^2) at various drawing speeds.